Correlating Microgeometry to Slicing Mechanics:

Design of a Simulated Ski Laceration Machine

A Major Qualifying Project Report

Submitted to the Faculty of

Worcester Polytechnic Institute

In partial fulfillment of the requirements for the

Degree of Bachelor of Science

By

Dylan Flegel

Richard Kern

Date:

December 16th, 2022

Report Submitted to:

Professor Christopher Brown

Worcester Polytechnic Institute

Abstract

The objective of this project is to investigate methods for understanding differences between hand and electrical side edge tuning of ski edges by examining the microgeometry and cutting performance of the edges. This paper discusses the design of a slicing machine, which will be used to conduct slicing tests with ski edges tuned with different sharpening methods. The findings may provide insight into how sharpening methods affect the risk of laceration injuries. The slicing machine has been constructed and is ready to begin conducting trials.

Acknowledgments

We would like to thank the WPI Surface Metrology Lab for providing the opportunity for this project and the WPI MQP Lab for providing access to 3D printers. We thank the WPI Ski Team for sharpening the ski edges. We also wish to thank Matt Gleason for providing Curfsoft, a software which will be used to analyze our ski edges during future work. We greatly appreciate the resources provided by Digital Surf, Sensofar, and Gel sight, which will also be used to measure and analyze our ski edges. Special thanks to Shu Guo for his continuous help with various aspects of this project.

Table of Contents

List of Tables

List of Figures

1. Introduction

1.1. Objectives

This project attempts to find a correlation between ski edge microgeometry and the slice it makes into a soft substrate. To accomplish this, our team requires a machine that can consistently slice a soft substrate with a ski edge. This machine will be used to acquire data on the depth of slice into a soft substrate. In future research, this data will be correlated to the microgeometry of each ski edge.

1.2. Rationale

It has been shown that lacerations caused by the edge of the ski can range between 5.6% to 33.6% of all skiing injuries, varying depending on the case study (Soares et. al 2022) (Holden et al. 2022). The incidence of these injuries on a larger scale is still being studied. While these lacerations are rare, they can be life-threatening (Holden et al. 2022). Laceration injuries caused by the edge of a ski involve direct damage to the skin and muscle. If these lacerations are deep enough, there is the risk of damaging nerves and arteries. This includes damage to the femoral artery and sciatic nerve in the lower body, and the radial artery and median nerve at risk in the upper body (Soares et. al 2022) (Holden et al. 2022).

Holden theorizes that the risk of these lacerations could increase due to new mechanical sharpening methods. Part of this claim is that these sharpening techniques give “a serrated nature” to the edge, which “may generate burrs and unwanted ridges” (Holden et al. 2022). While this claim has not been proven, research has shown that blades with micro-serrations experience increased forces during slicing while also cutting deeper into soft material (Giovannini and Ehmann 2016). By studying how the microgeometry of a ski edge affects its slicing performance, insight into what microgeometries may be affecting the severity of laceration injuries could be provided.

1.3. State of the Art

1.3.1. Mechanics of slicing

A laceration is “a pattern of injury in which skin and underlying tissues are cut or torn” (Newman and Mahdy 2022), and can be caused by a wide variety of mechanisms. Ski lacerations, in this case, specifically refer to injuries caused by a ski edge cutting the skin and underlying tissue.

Looking into the mechanics of cutting, Brown posits that there are three types of cutting: chopping, slicing, and scraping. Like many real-world instances of cutting, ski lacerations can be a combination of all three cutting types. Predominantly, however, the mechanism of these lacerations can be described as slicing.

Slicing has been defined as a reduction in cutting force caused by motion parallel to the cutting edge. To explore the mechanics behind this reduction, Atkins defined the slice-push ratio (Atkins et. al 2004). This is the ratio between the speed of motion parallel to the edge (slice), and the speed of motion perpendicular to the edge (push). Normalizing the cutting forces to the fracture toughness of the soft substrate, an analysis of the effect of this slice push-ratio on these forces could be completed. This analysis demonstrated that a linear increase in the slice-push ratio results in a non-linear reduction of the perpendicular cutting force. Additionally, it was found that the parallel cutting force increased as the slice-push ratio approached 1. After peaking at a ratio of 1, the parallel cutting forces slowly decreased in response to an increased slice-push ratio. Overall, this study was able to classify slicing through this slice-push ratio. The ratio was then used to demonstrate the role of slicing in reducing the cutting forces required to cut a soft substrate.

Isolating the role of the slice-push ratio in the reduction in cutting forces has allowed further research into other factors that affect cutting force. As an example, there is the conclusion that the angle between an edge and its direction of motion can reduce cutting forces. This was found by comparing the expected reduction by the slice-push ratio to the measured reduction at various angles (Spagnoli et. al 2019).

1.3.2. Correlation of edge microgeometry to cutting performance

Microgeometry is a term specified by Denkena and Biermann to describe an edge. Specifically, microgeometry refers to all geometric detail that falls within the intersection between the two faces of an edge (Denkena and Biermann 2014). A visual representation of this definition is shown in Figure 1.

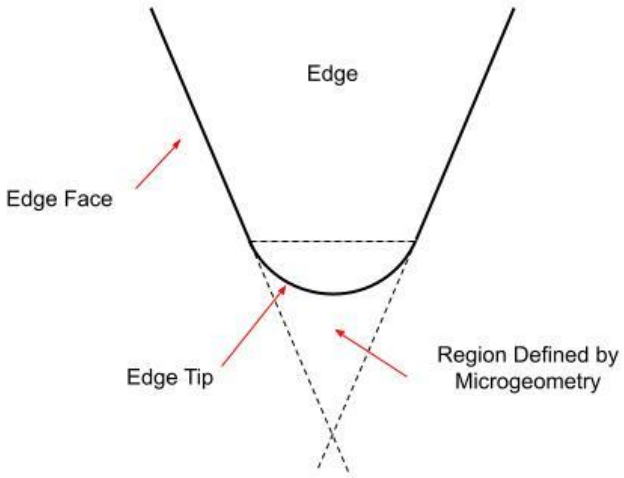

Figure 1: Microgeometry as Specified by Denkena and Biermann

Investigations correlating edge microgeometry to scraping performance have been well documented. For scraping, edge performance refers to the resulting chip formation, with the desired outcome varying for each study. This research has shown that microgeometry determines all aspects of scraping mechanics, including cutting parameters, tool parameters, and scraping procedure (Denkena and Biermann 2014).

The correlation of edge microgeometry to chopping performance has been investigated. While a standardized definition of chopping performance has not been generally accepted, McCarthy proposed the use of a Blade Sharpness Index (BSI). This value is determined by measuring both edge displacement and cutting force required to initiate a cut into a soft substrate with known fracture toughness and thickness (McCarthy et. al 2007). Additionally, the cutting force can be written as a function of displacement once empirical constants are determined for a given material. The resulting measurement is independent of substrate properties, allowing further research to be done into what edge microgeometries affect BSI. Of the variables studied, it was found that the tip radius of an edge has the biggest impact on BSI. While the existence of a correlation was determined, further research is needed to correlate cutting performance to microgeometry independent of measurement scale (McCarthy et. al 2010).

Correlations have been found relating microgeometry to both scraping and chopping performance. However, this is not the case for slicing. While research has been done into the mechanics of slicing, no correlation between edge microgeometry and slicing performance has been found (Deibel et. al 2013, Porazzo et. al 2017). Despite this lack of

decisive evidence, the fact that other mechanisms of cutting are directly affected by edge geometry suggests that such a correlation does exist.

1.4. Approach

Evidence that certain ski sharpening methods can increase the severity of laceration injuries has yet to be found. This is due to the lack of general evidence correlating edge microgeometry to slicing performance, despite the fact that edge microgeometry directly influences the performance of other cutting mechanisms. In order to investigate whether such a correlation exists, a machine was developed to slice a substrate with a given ski edge.

Throughout this project, we had access to a variety of different ski edges. During our design process, we decided to focus on a set of ski edge segments. These segments were part of a previous research project for the WPI Surface Metrology Lab. This meant that the ski segments were cut, sharpened, and measured prior to the start of our project. The sharpening process for each segment was documented, as each segment was sharpened with a different method. This included both hand and machine sharpening methods. The resulting topography of each ski edge segment was then measured with a Sensofar S Neox 3D optical profiler microscope.

Axiomatic Design was used to develop both the slicing machine and the substrate. This process involved following the two core axioms defined by Suh (2001). The first axiom is maintaining independence. By establishing design requirements and solutions that are each independent from one another, elements of the resulting design can be easily adjusted. This is because adjusting one element will not infringe on separate elements of the design. Suh's second axiom is minimizing information. This helps ensure simplicity in the final design, maximizing its probability of success.

1.5. Methods

An integral part of the Axiomatic Design process is the creation of a design decomposition table. As suggested by the name, this table decomposes the design process into a hierarchical structure. This ensures each requirement and solution of the design is listed simply and independently, following both main axioms. Within this decomposition table, Functional Requirements (FRs) specify design challenges that need to be solved, while Design Parameters (DPs) specify solutions to these challenges.

The first step in developing a design decomposition is the identification of customer needs (CN). The FRs are developed to address the CN. The overarching goal of this research project is to inform skiers on what edge-sharpening methods may increase the laceration severity, if any. We also aim to contribute to research on slicing mechanics. Research regarding slicing mechanics relates to medical tool design and food processing, to name two examples.

Once the customer needs were identified, we could outline a decomposition aimed at fulfilling these needs. This started with the formulation of FRs, which were split into a variety of subsections to ensure information would be minimized, while still being collectively exhaustive. After these FRs were formulated, DPs specifying all of our design options to satisfy each FR were brainstormed. This was then paired down to have one DP for each FR. The resulting design decomposition is shown in Table 1. Our reasoning behind each FR and DP, along with the fabrication process for each DP, is listed in the “Design Process” section.

Table 1: Axiomatic Design Decomposition

			Functional Requirement				**Design Parameter**
FR1			Fabricate a soft substrate to be sliced	DP1			Gel approximation of skin
	FR1.1		Mix Gel		DP1.1		Scale to measure mass of water and gelatin
	FR1.2		Cast gel		DP1.2		Baking tray
	FR1.3		Incorporate gel into slicing machine		DP1.3		Gel segments cut to size

FR2			Create relative displacement between the gel and ski edge	DP2			Machine that moves the gel along ski edge
	FR2.1		Hold gel on ski edge		DP2.1		Housing for substrate
		FR2.1.1	Allow gel to move into ski edge			DP2.1.1	Inner housing that can slide vertically within housing
		FR2.1.2	Reproduce vertical force between ski edge and gel			DP2.1.2	Weights on top of substrate
		FR2.1.3	Visualize depth of slice into gel			DP2.1.3	"Window" in housing used to determine vertical displacement
		FR2.1.4	Attach a string to the housing			DP2.1.4	Two anchor points on either side of the housing
	FR2.2		Secure ski to system		DP2.2		Ski holder
	Constraint 2.2.0		friction force between the substrate and ski edge must be measurable				
		FR2.2.1	Hold ski at a 45° angle			DP2.2.1	Angled base for ski holder to rest on
		FR2.2.2	Accommodate ski edges with different length			DP2.2.1	Skis are cut to a specific length
		FR2.2.3	Level ski			DP2.2.3	Adjustable mount for ski
		FR2.2.4	Measure friction between base and holder			DP2.2.4	Force gauge and holder
		FR2.2.5	Mitigate friction between base and holder			DP2.2.5	Indentation to reduce contact area
	FR2.3		Create a reproducible displacement of slice		DP2.3		Stepper motor and winch system
		FR2.3.1	Connect motor to the housing			DP2.3.1	Housing secured to a spool on the motor with string
		FR2.3.2	Increase stability of housing			DP2.3.2	Two guide rails and brackets
		FR2.3.3	Secure the motor to the system			DP2.3.3	Acrylic laser cut stand
		FR2.3.4	Make housing adjustable based on ski thickness			DP2.3.4	Sliding connection between housing and rail
		FR2.3.5	Secure each part to the system			DP2.3.5	Base where all the mounts are attached
		FR2.3.6	Control displacement of housing			DP2.3.6	Code controlling number of steps
	FR2.4		Measure the friction force between gel and ski edge		DP2.4		Secured force gauge that connects to ski holder

2. Design Process

2.1. Design Overview

The design is divided into two major FRs: fabricating a soft substrate, and creating a displacement between the soft substrate and a ski edge. A medical model was used to approximate the material properties of skin. The model was a 33% gelatin powder to water ratio measured by weight, and was used in previous research to test needle indentation below the epidermis layer (Moronkeji et. al 2017). To create the necessary displacement, a slicing machine was designed to move this substrate across a given ski edge. The final design for the slicing machine is shown in Figure 2.

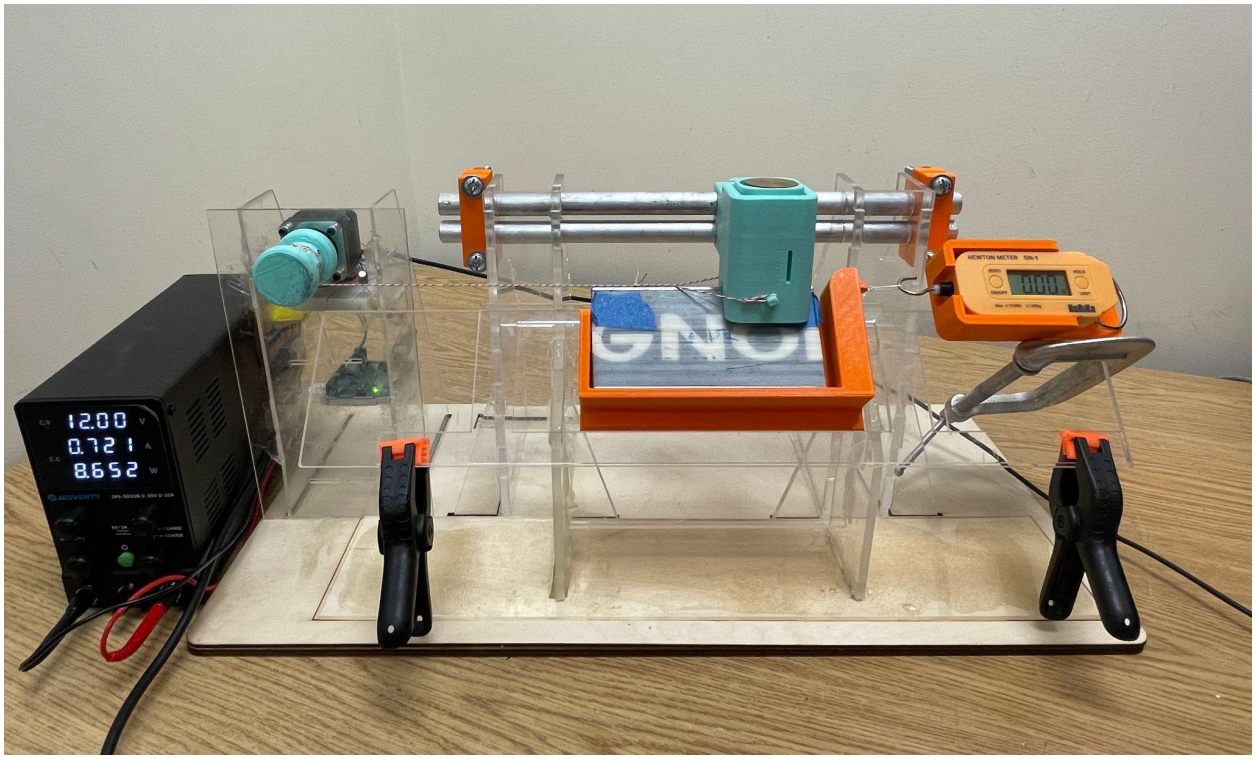

Figure 2: Slicing Machine

2.2. Soft Substrate

2.2.1. FR1.1-FR1.2 and DP1.1-DP1.2

The substrate used is measured by percent weight. The desired thickness of this gel is 1cm, meaning that 71mL of gelatin mixture was required to cast in the selected 2.5”x5” tray. At this volume, 31g of gelatin powder was needed. To fully dissolve gelatin powder into the water, the water was first brought to boiling temperature. A scale was then

used to measure 71g of this water before the gelatin powder was mixed in. Before the mixture could cool, it was poured into a 2.5”x5”

2.2.2. FR1.3 and DP1.3

The substrate is cast in a 2.5in x 5in tray, so it must be cut into smaller sections. The gel is cut to 1in x 1in sections, allowing for about 10 sections of substrate for each cast. To ensure there is a tight fit, the sections are cut to be slightly longer than 1”. The gel sections are then trimmed to size.

2.3. Slicing Machine

FR2.1 and DP2.1 - Gel Housing

The machine will pull the substrate over the ski edge. This requires a method of keeping the fabricated gel in contact with the ski edge. To accomplish this, we designed a housing for the gel. The final CAD model of the gel housing is shown below in Figure 3 and Figure 4.

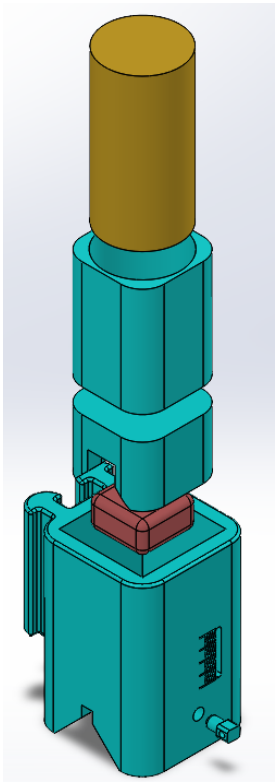

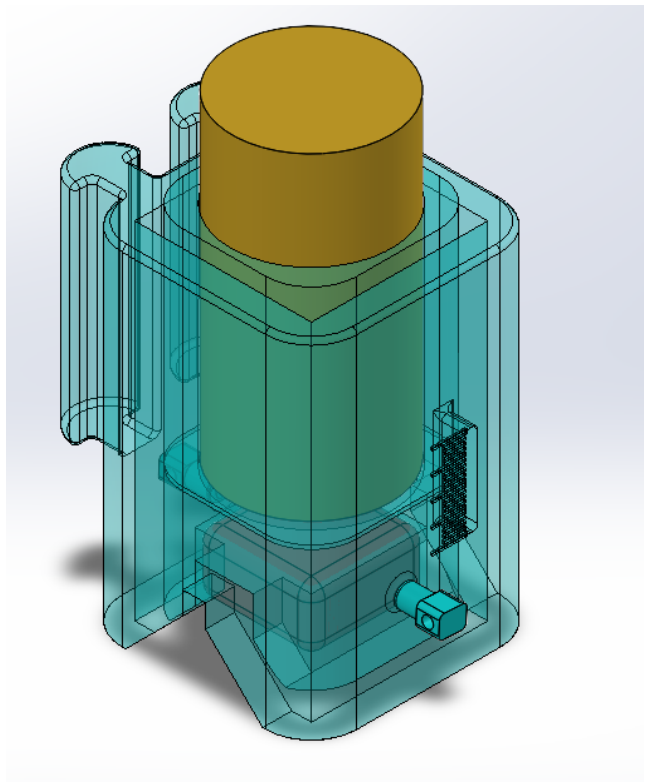

Figure 3 (Left): Housing Exploded View

Figure 4 (Right): Housing Assembled View

2.3.1.1. FR2.1.1 and DP2.1.1

FR 2.1.1. requires the substrate to be able to move into the ski. If the distance between the substrate and ski edge is fixed, the edge would not be able to slice deeper into the gel. Our solution was to design an inner housing that holds the substrate and sits in an outer housing. The inner housing has a 1” x 1” compartment, allowing the substrate to be press-fit into the holder. This inner housing is able to move vertically within the outer housing.

2.3.1.2. FR2.1.2 and DP2.1.2

Slicing requires a force between the edge and substrate. This was created using a weight on top of the inner housing. The weight we used was a brass cylinder with a mass of 460g. An additional part was designed to hold the weight. This weight holder ensures the cylinder is over the center of the substrate.

2.3.1.3. FR2.1.3 and DP2.1.3

The machine requires a way to measure how deep the edge slices into the substrate. To achieve this, a window was created in the outer housing. Beside the window is a set of marks, each one millimeter apart from each other. The marks can be used to measure the height of the gel. The line between the inner housing and the weight holder can be used to determine the displacement of the inner housing. This is done by measuring the line’s height before and after the trial and calculating the difference. The window is shown in Figure 5.

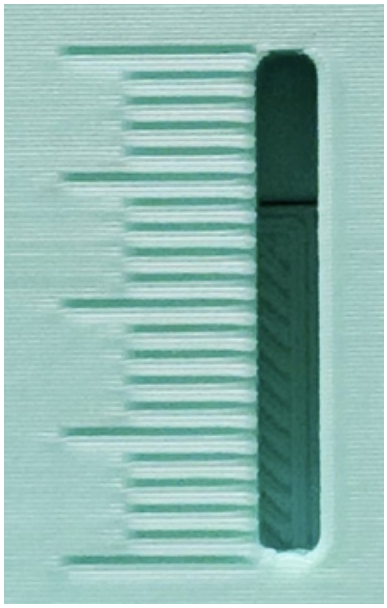

Figure 5: Outer Housing Window

2.3.1.4. FR2.1.4 and FR2.1.4

The force pulling the housing must be at the same height as the edge. If the housing was pulled from the top there would be a moment about the housing, resulting in uneven pressure across the gel. The solution was to have two anchor points on either side of the housing. This allowed the anchors to be placed at an appropriate height and not interfere with the edge. Two holes were created on the sides of the housing and anchors were press-fit into the holes.

2.3.2. FR2.2 and DP2.2 - Ski Holder

To slice with a ski edge, we need a method of securing these skis to our machine. This must be achieved while also allowing for the friction force generated between the gel and the ski to be measured. Our solution was to design a holder for the ski that can slide parallel to the slicing motion.

2.3.2.1. FR2.2.1 and DP2.2.1

To create a slice on ski edges, the tip of the edge must be oriented vertically. The ski edges were sharpened at a 90° degree angle between the base and the side edge. To orient the tip of each edge vertically, the ski holder rests on an acrylic base angled 45° from flat.

2.3.2.2. FR2.2.2 and DP2.2.2

FR2.2.1 required that the machine be compatible with any 90° degree ski edge to reduce the limitations of what ski edges can be measured. This means that a method is required to fit these edges into our machine, while also keeping within the constraint that friction must be measurable. Measuring the friction on full-length skis was determined to be impractical for the scope of our project. Our solution was to cut ski edges to length. This allows us to satisfy the requirement of testing any ski edge while keeping within the constraints of our design

2.3.2.3. FR2.2.3 and DP2.2.3

In order to properly measure the change in depth, FR2.2.2 specifies that the angle of the ski edge must be level. The edge of a ski is not a straight line, so if the ski rests flat on its side, the depth measurement will vary at different spots on the edge. To account for this, the ski mount was made to be adjustable. This mount is secured to the base with clamps, allowing it to be moved to the proper orientation between trials. The mount is properly leveled by placing the housing at one end of the ski edge without the gel and reading the depth measurement using the window discussed in FP2.1.3. The housing is then moved to the other end of the ski edge, with the mount angle adjusted such that the depth measurement matches the first depth measurement. This ensures the ski edge depth is consistent throughout the displacement.

2.3.2.4. FR2.2.4-FR2.2.5 and DP2.2.4-DP2.2.5

The friction between the gel and the ski edge must be measurable. By designing the ski holder to rest on the acrylic base, the holder is free to slide horizontally. A loop on the side of the ski holder can then be secured to a force gauge, which measures the horizontal force on the ski during each trial. To increase the accuracy of this measurement, FR2.2.5. specifies that the other frictions in the system should be reduced. The biggest source of friction other than the gel is between the ski holder and the base. To reduce the friction caused by the ski holder, the bottom surface of the holder was designed to only rest on its top and bottom edges (surface area is ⅛” thick for each).

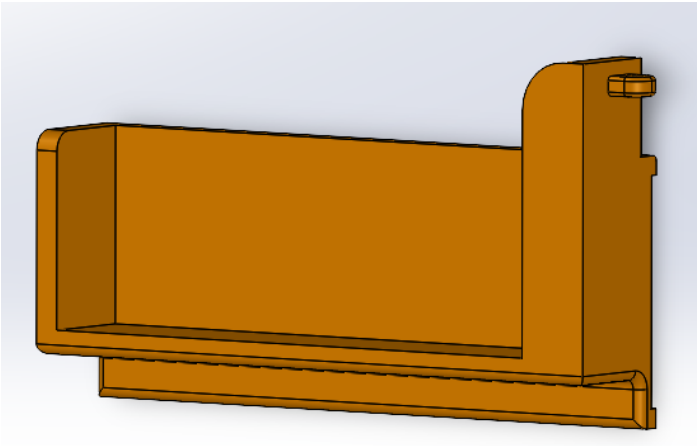

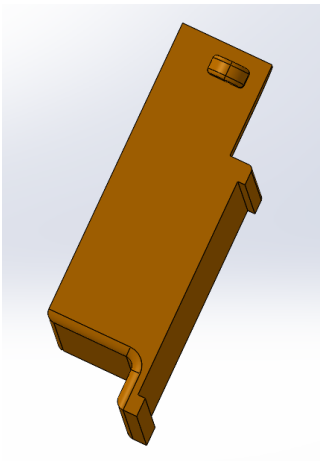

Figure 6 (Left): Force Gauge Holder Front View

Figure 7 (Right): Force Gauge Holder Side View

2.3.3. FR2.3 and DP2.3- Moving the housing

2.3.3.1. FR2.3.1 and DP2.3.1

A stepper motor and winch system is used to pull the housing and create a consistent displacement. The stepper motor is connected to the housing using a spool and string. The motor is supported by an acrylic mount. The housing is pulled towards the stepper motor when the motor is running. The stepper motor, spool, and motor mount are shown in Figure 8.

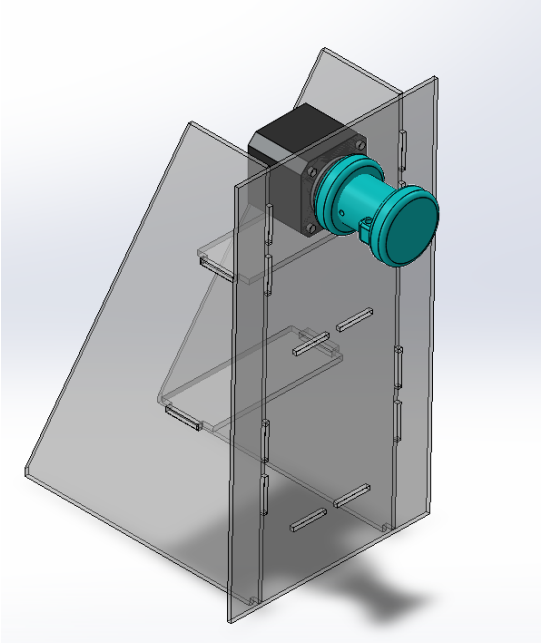

Figure 8: Motor Mount and Spool

2.3.3.2. FR2.3.2-FR2.3.3 and DP2.3.2-DP2.3.3

The housing must be stable when being pulled by the motor. To address this, a rail guide system was made for the housing to slide along. The system is made of two aluminum bars. There are two bars, as having only one would allow the housing to rotate. The rail system is supported by two acrylic mounts, which hold the bars at either end. The bars are held at the same height as the holder. A pair of clamps are attached at either end of the bars to prevent the bars from sliding.

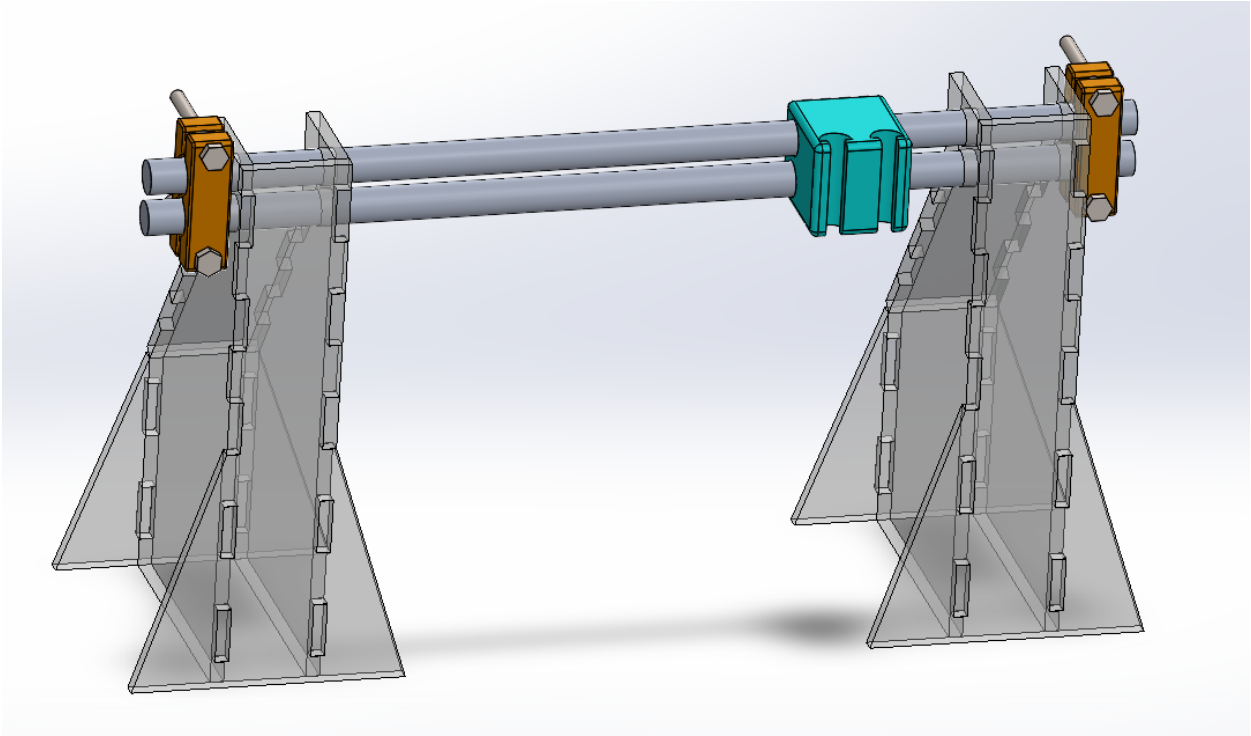

Figure 9: Rail System

2.3.3.3. FR2.3.4 and DP2.3.4

The ski segments that will be used for the trials differ in width. As a result, the height of the housing will change depending on the width of the ski segment. To account for this, a connector piece was made that attaches to the housing and the rails with a tight fit. This allows the housing to be able to slide vertically within the connector piece, with friction allowing it to be set to differing heights.

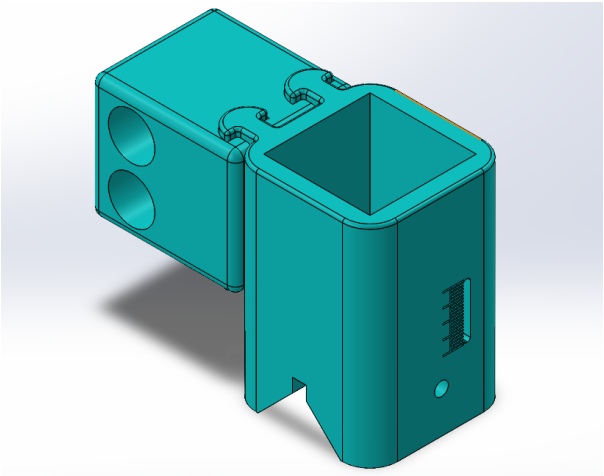

Figure 10: Outer Housing and Rail Connector

2.3.3.4. FR2.3.5 and DP2.3.5

The acrylic ski holder, motor mount, and rail mounts must all be secured so they do not move during the trials. A base was made for all of the components to be attached to. The base is composed of two layers of baltic birch plywood. Slots were cut into the top layer that holds the components in place. The bottom layer is a solid sheet of wood. The two layers were glued together, and the components were glued onto the base. The two layers are shown in Figure 11.

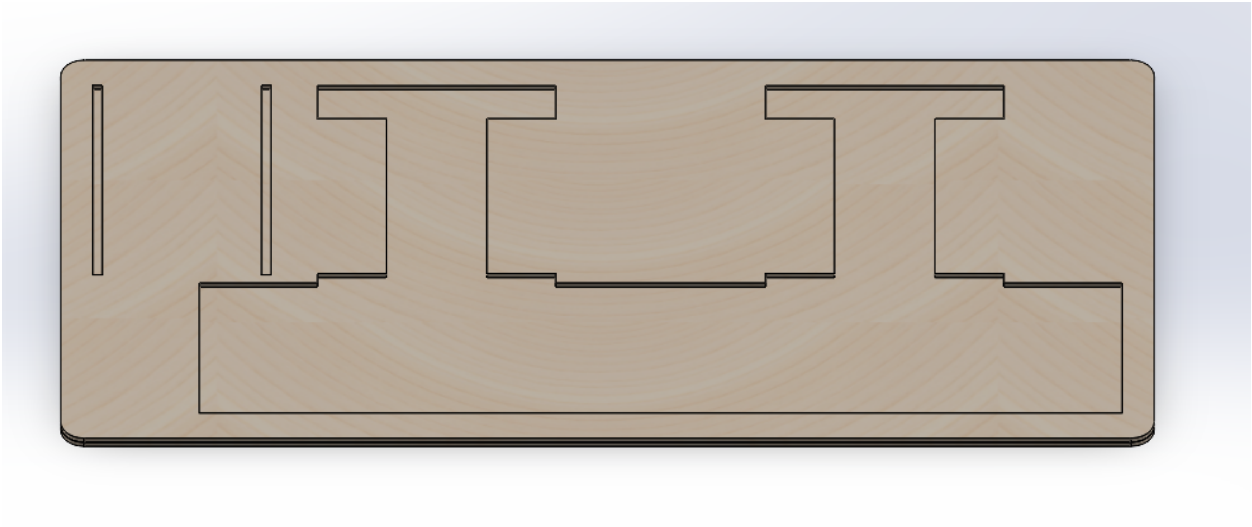

Figure 11: Machine Baseplate

2.3.3.5. FR2.3.6-FR2.3.7 and DP2.3.6-DP2.3.7

A program was made to allow an Arduino to control the stepper motor. FR2.3.6 requires the displacement of the housing to be controlled. A variable in the program is able to control the number of steps the stepper motor makes. FR2.3.7 requires the velocity of the motor to be controlled. There is a variable in the program that controls the duration of each step. Increasing the delay will decrease the speed of the motor. The code is shown in Appendix A.

2.3.3.6. FR2.3.8 and DP2.3.8

FR2.3.8 requires power to be provided to the stepper motor. An A4988 Stepper Motor Driver is used to allow the Arduino to control the stepper motor. The Arduino has a 5V output to power the motor driver. An adjustable power supply is used to power the motor. The external power supply is set to 12V.

2.3.4. FR2.4 and DP2.4- Measuring the Friction Force

The friction between the gel and the ski should be measured. To measure the friction force, a force gauge was tied to the ski holder. When the gel slides across the ski, the friction pulls the ski toward the motor. The ski pushes onto the ski holder and the force is registered in the force gauge. A holder was designed to secure the force gauge to the acrylic base (seen in Figure 2). Digital Newton Meter from Arbor Scientific was selected due to its compact nature. Video analysis of this gauge demonstrated a response time of 210ms. A camera will be used to record displayed friction force during the test.

3. Testing and Alternate Designs

3.1. Substrate

There were multiple candidates for the substrate. Wax was initially used, but testing showed that the mechanism would result in scraping instead of slicing. Our test requires a soft body material to test slicing. The next candidate was a silicon substrate that approximated skin by incorporating multiple layers. Silicone gels (Ecoflex Dragon Skin 10 and Ecoflex 30) were used (Williams et. al, 2020), however, these gels proved too tough for the machine to slice. The team's next plan was to use a layered gelatin and agar substrate demonstrated by Chen and Balter (2016). However, replicating this process proved to be out of the scope of this project due to the high gelatin to water ratios it required. Next, we

attempted to create a substrate using only gelatin and water. We created multiple gels with different concentrations of gelatin and water by volume. We tested substrates with a 20% gelatin ratio (Monrokeji, 2017), a 33% gelatin ratio (Monrokeji, 2017), and a 50% gelatin ratio. The 20% gelatin substrate would crumble during tests and the 50% gelatin substrate was too tough to be sliced. The 33% gelatin was able to be sliced.

There were also different approaches to casting the substrate. Individual molds were initially used. To do this, tubes with a 1” diameter were 3D printed and glued to a piece of acrylic. The adhesive prevented the gel from leaking from the bottom. The tubes were filled with gel layers and left to cure. Once cured, the tubes were pulled off to break the adhesive and the gels were removed. Controlling the thickness of the gel required precise volume measurements. We were unable to measure the volume with the required precision, as pouring a mixed viscous gel would result in material adhering to the measuring container. The next method was to cast the gel as a sheet in a baking tray. When the gel solidified, squares could be cut and removed from the tray. This approach using larger volumes reduced the impact of the losses discussed in the previous method.

3.2. Slicing Machine

3.2.1. Housing

Initially, the inner housing was 3D printed in the same orientation as the outer housing, as shown in Figure 11. Testing showed that layered grooves between the inner and outer housing were catching, causing friction and resulting in an inconsistent vertical force on the gel. The inner housing was reprinted on the plane perpendicular to the outer housing, shown in Figure 12.

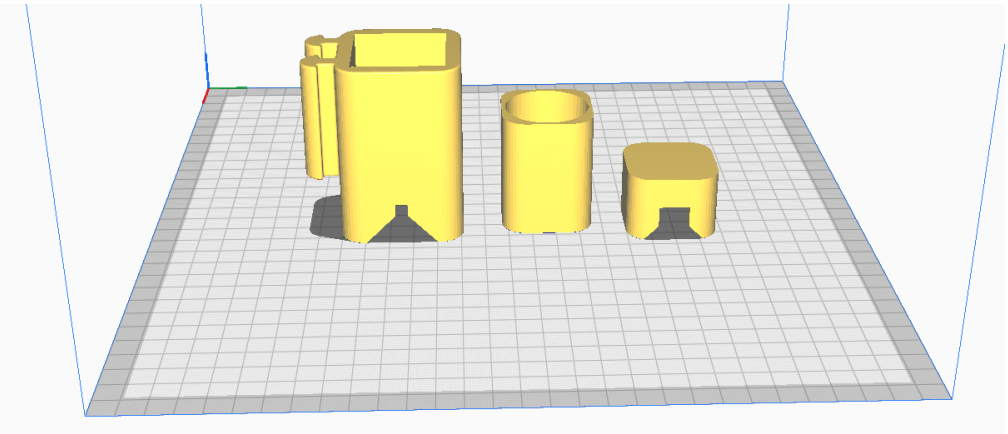

Figure 12: Initial 3D Printing Orientation of Housing

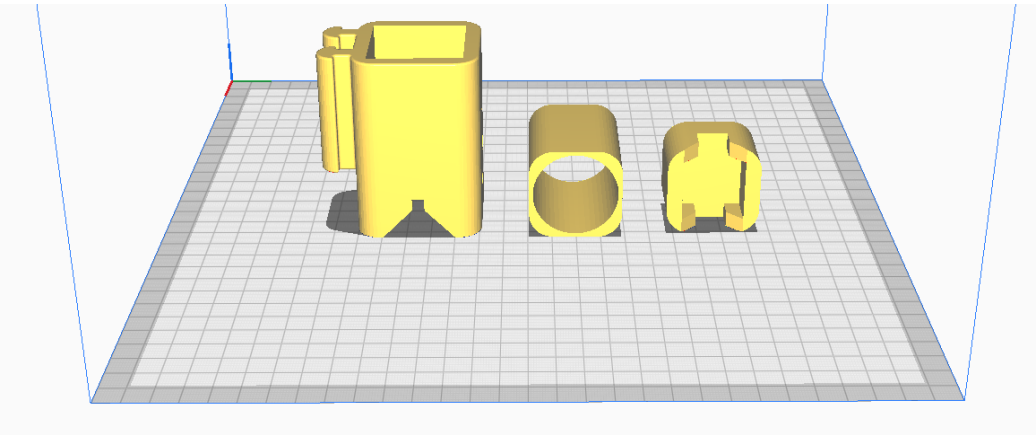

Figure 13: Final 3D Printing Orientation of Housing

3.2.2. Securing Ski

Initial design involved clamping the ski directly to the ski holder. This was redesigned, however, to allow the ski to slide along the holder. When this was changed, we realized our sled-mounted force holder (Figure 14) relied on securing the ski. This was redesigned to decouple force gauge mounting from ski mounting. The force gauge sled on a clamped ski design is shown in Figure 14.

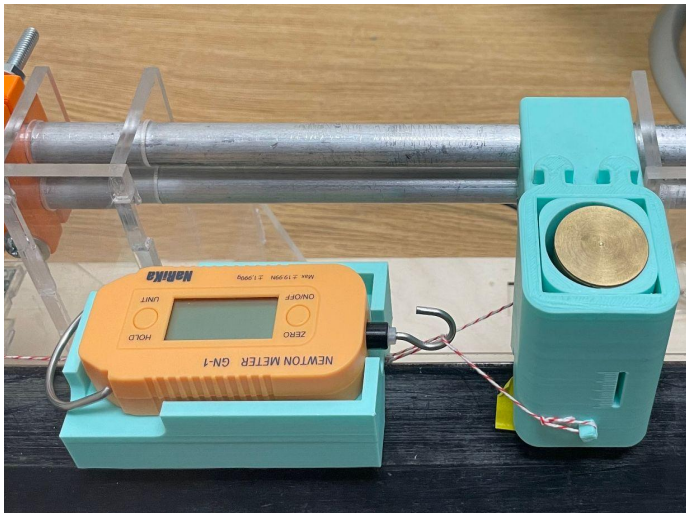

Figure 14: Initial Force Gauge Holder

3.2.3. Power Supply

A power supply with 12V and 5A was initially used. The circuit would occasionally not work with this setup. It was determined that 5A was too much current for the motor

controller. The power supply was replaced with a power supply where the amperage and voltage can be adjusted.

3.2.4. Rail

Brackets were designed to prevent the rail from sliding. The first bracket design is shown in Figure 15. This included a spacer to keep the distance between these bars consistent while tightening these brackets. Testing showed that the bars were still pushed apart, with the housing unable to move along the rail while the brackets were secured. Adjusting this design would require fine-tuning the tolerances for this middle spacer. A new bracket was designed to put pressure on the sides of the bar, meaning the design did not have to rely on a middle bracket.

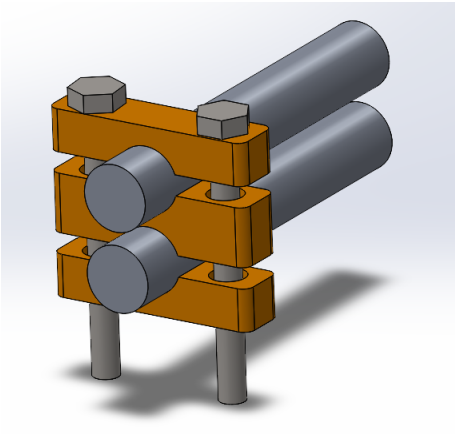

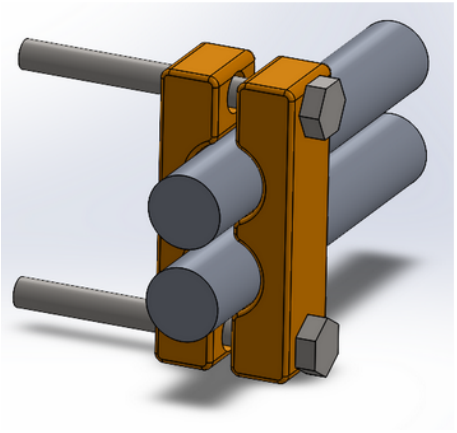

Figure 15 (Left): Initial Bracket Clamp Design

Figure 16 (Right): Final Bracket Clamp Design

4. Discussion

4.1. Final Design Conclusions

Testing procedures have shown that each parameter of our design fulfills its functional requirement. The slicing machine is able to produce a consistent displacement of a soft substrate along a ski edge segment. Furthermore, it can slice a 33% gelatin substrate.

One procedure that must be addressed before conducting trials is the lubrication of the ski edge. During our tests, the friction between the gel and ski edge would sometimes

cause the gel to fold, resulting in an uneven slice. The lubrication will hopefully mitigate this issue as the lubrication of an edge is known to decrease the force required to slice a material. It is common practice for ski racers to lubricate their edges, so this adjustment will also make the ski edge topography more similar to real-world conditions.

4.2. Continuation

In the future, our team will use the slicing machine to conduct trials with 7 different ski segments. The results from these trials will then be compared to the microgeometry of the ski edges. This will be done by analyzing the measurements made with Sensofar's S Neox 3D optical profilometer. Several methods will be used for this analysis, with the goal of differentiating the edges sharpened with mechanical methods and the edges sharpened by hand. There are two broad approaches planned for analyzing the edge: profile analysis and cross-section analysis.

Profile analysis examines the line running across the peak of an edge. This profile is found by finding the highest points at the top and bottom of the topography map. A line is drawn between the two points, which generates a two-dimensional plot of the ski edge profile. The profile graph is then leveled before the analysis is performed. A topography map is shown in Figure 16, and the resulting leveled profile is shown in Figure 17.

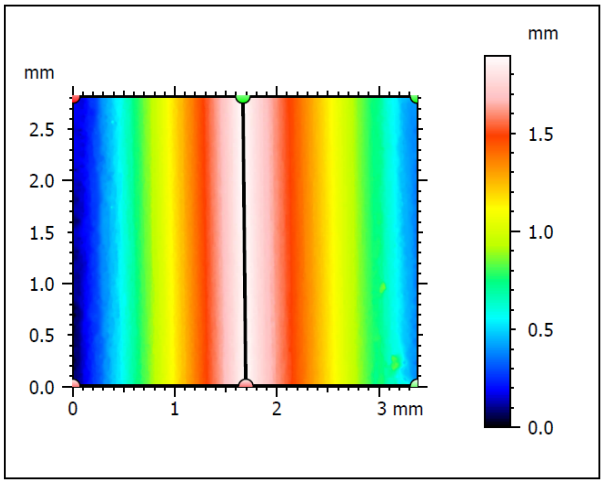

Figure 17: Example Topography Map with Profile

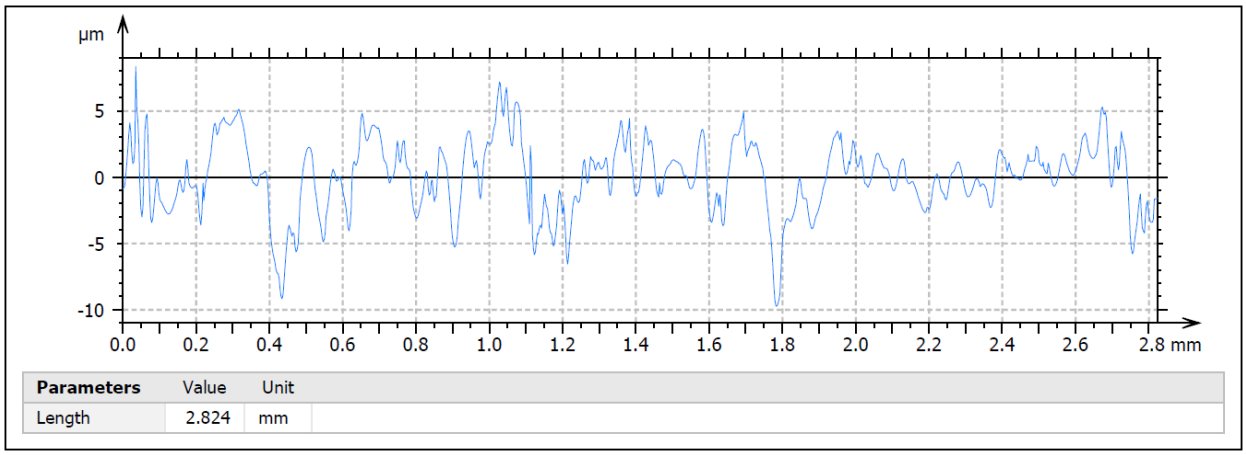

Parameters	Value	Unit
Length	2.824	mm

Figure 18: Example Ski Edge Profile

There are two different analysis methods that will be used to analyze the edge profile: length scale analysis (LSA) and power spectral density (PSD). The example profile shown in Figure 17 is used to create an LSA graph, shown in Figure 18, and a PSD graph is shown in Figure 19.

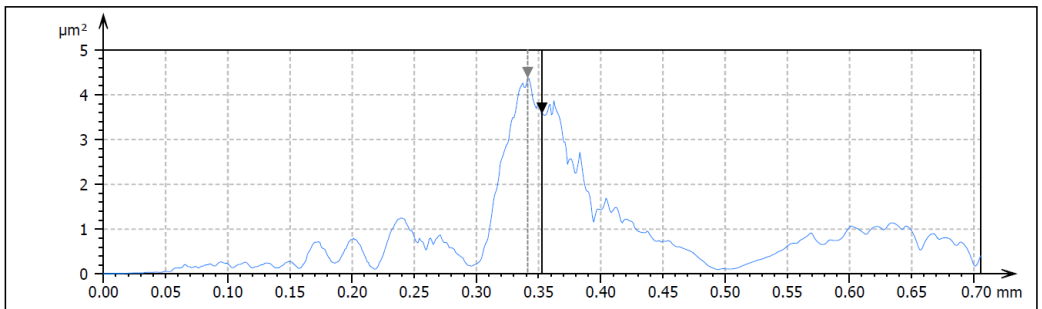

Information	
Zoom factor	x4
# of iterations	32
Smoothing	11
Window function	None

Parameters	Value	Unit
Wavelength	0.3533	mm
Amplitude	1.889	µm
Dominant wavelength	0.3413	mm
Maximum amplitude	2.090	µm

Figure 19: Example Length Scale Graph

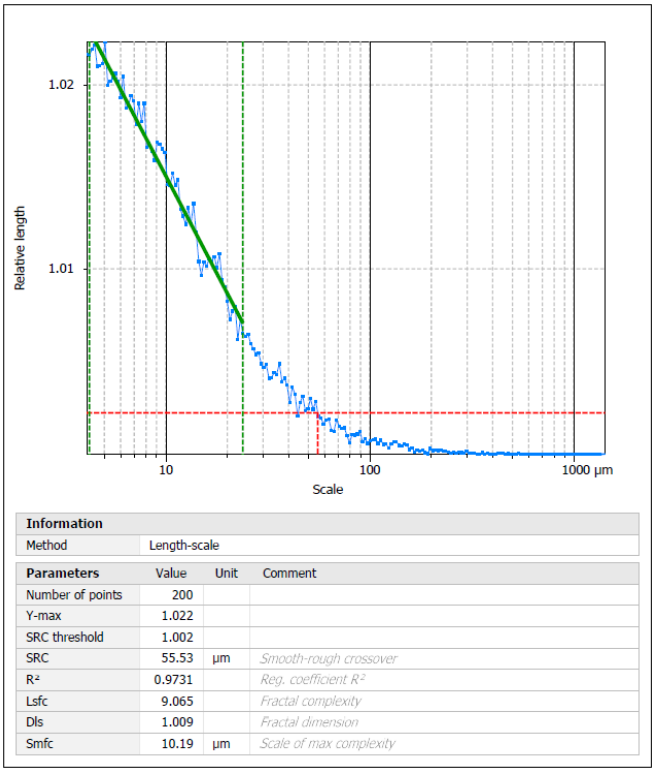

Information	
Method	Length-scale

Parameters	Value	Unit	Comment
Number of points	200		
Y-max	1.022		
SRC threshold	1.002		
SRC	55.53	µm	*Smooth-rough crossover*
R^2	0.9731		*Reg. coefficient R^2*
Lsfc	9.065		*Fractal complexity*
Dls	1.009		*Fractal dimension*
Smfc	10.19	µm	*Scale of max complexity*

Figure 20: Example Power Spectral Density Graph

Cross-sectional analysis examines a cross-section slice of the edge. An example of a cross-section is shown in Figure 20. These cross-sections will be analyzed using multiscale curvature analysis. A multiscale curvature analysis graph is shown in Figure 21.

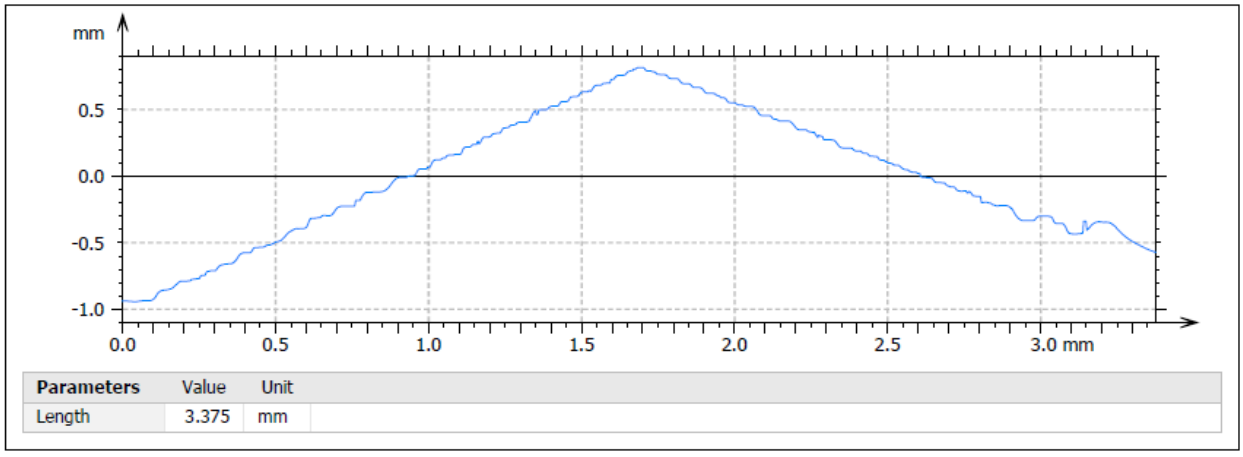

Parameters	Value	Unit
Length	3.375	mm

Figure 21: Example Cross-Section

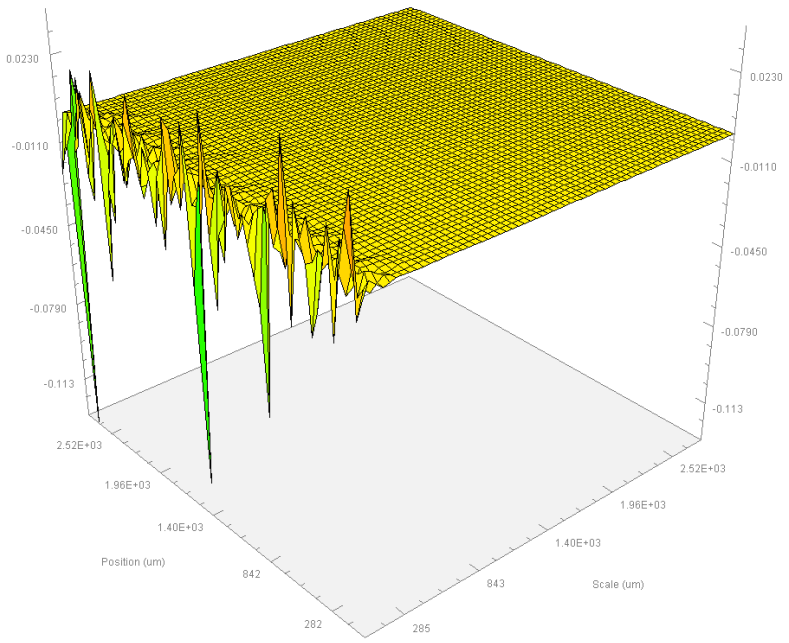

Figure 22: Example Multiscale Curvature Analysis Graph

5. References

Chen, Alvin I., Max L. Balter, Melanie I. Chen, Daniel Gross, Sheikh K. Alam, Timothy J. Maguire, and Martin L. Yarmush. "Multilayered Tissue Mimicking Skin and Vessel Phantoms with Tunable Mechanical, Optical, and Acoustic Properties." Medical Physics 43, no. 6Part1 (June 2016): 3117–31. https://doi.org/10.1118/1.4951729.

Deibel, Karl-Robert, Christian Raemy, and Konrad Wegener. "Modeling Slice-Push Cutting Forces of a Sheet Stack Based on Fracture Mechanics." Engineering Fracture Mechanics 124–125 (July 2014): 234–47. https://doi.org/10.1016/j.engfracmech.2014.04.029.

Denkena, B., and D. Biermann. "Cutting Edge Geometries." CIRP Annals 63, no. 2 (2014): 631–53. https://doi.org/10.1016/j.cirp.2014.05.009.

Giovannini, Marco, and Kornel Ehmann. "Vibrational Cutting of Soft Tissue with Micro-Serrated Surgical Scalpels." Procedia CIRP 45 (2016): 199–202. https://doi.org/10.1016/j.procir.2016.02.342.

Holden, William M., Michael S. Barnum, Mitchell C. Tarka, Christoph A. Niederhauser, Ryan P. Jewell, and Nathan K. Endres. "Severe Lacerations in Alpine Ski Racing: A Case Series and Review of the Literature." Sports Health: A Multidisciplinary Approach, March 31, 2022, 194173812210765. https://doi.org/10.1177/19417381221076521.

McCarthy, C.T., A. Ní Annaidh, and M.D. Gilchrist. "On the Sharpness of Straight Edge Blades in Cutting Soft Solids: Part II – Analysis of Blade Geometry." Engineering Fracture Mechanics 77, no. 3 (February 2010): 437–51. https://doi.org/10.1016/j.engfracmech.2009.10.003.

McCarthy, C.T., M. Hussey, and M.D. Gilchrist. "On the Sharpness of Straight Edge Blades in Cutting Soft Solids: Part I – Indentation Experiments." Engineering Fracture Mechanics 74, no. 14 (September 2007): 2205–24. https://doi.org/10.1016/j.engfracmech.2006.10.015.

Moronkeji, K., S. Todd, I. Dawidowska, S.D. Barrett, and R. Akhtar. "The Role of Subcutaneous Tissue Stiffness on Microneedle Performance in a Representative in Vitro Model of Skin." Journal of Controlled Release 265 (November 2017): 102–12. https://doi.org/10.1016/j.jconrel.2016.11.004.

Newman, R. K., & Mahdy, H. (2022, October 8). "Laceration." National Center for Biotechnology Information. Retrieved December 12, 2022, from https://www.ncbi.nlm.nih.gov/books

Porrazzo, J., Sheahan, M., and Spear, S. (2017). "Analysis of Edge Curvature and Roughness in Slicing. Major Qualifying Project." Worcester Polytechnic Institute.

Soares, Sérgio, Timo Schmid, Lucien Delsa, Nicolas Gallusser, and Beat K. Moor. “Skiing and Snowboarding Related Deep Laceration Injuries. A Five-Season Cross-Sectional Analysis from a Level-1 Trauma Centre in the Swiss Alps.” Orthopaedics & Traumatology: Surgery & Research 108, no. 7 (November 2022): 103370. https://doi.org/10.1016/j.otsr.2022.103370.

Spagnoli, A., R. Brighenti, M. Terzano, and F. Artoni. “Cutting Resistance of Soft Materials: Effects of Blade Inclination and Friction.” Theoretical and Applied Fracture Mechanics 101 (June 2019): 200–206. https://doi.org/10.1016/j.tafmec.2019.02.017.

Suh (2001). “Axiomatic Design: Advances and Applications.” Oxford University Press, 2001, ISBN 0-19-513466-4

Williams, Taylor P., Clifford L. Snyder, Kevin J. Hancock, Nicholas J. Iglesias, Christian Sommerhalder, Shannon C. DeLao, Aisen C. Chacin, and Alexander Perez. “Development of a Low-Cost, High-Fidelity Skin Model for Suturing.” Journal of Surgical Research 256 (December 2020): 618–22. https://doi.org/10.1016/j.jss.2020.07.051.

Appendix A: Stepper Motor Code

```
#define dirPin 2
#define stepPin 3
#define numberOfSteps 225
#define stepDuration 2500

void setup() {
  // Declare pins as output:
  pinMode(stepPin, OUTPUT);
  pinMode(dirPin, OUTPUT);
}

void loop() {
  // Set the spinning direction clockwise:
  digitalWrite(dirPin, LOW);

  for (int i = 0; i < numberOfSteps; i++) {
            // These four lines result in 1 step:
            digitalWrite(stepPin, HIGH);
            delayMicroseconds(stepDuration);
            digitalWrite(stepPin, LOW);
            delayMicroseconds(stepDuration);
  }

delay(1000);

  digitalWrite(dirPin, HIGH);
  for (int i = 0; i < numberOfSteps; i++) {
            // These four lines result in 1 step:
            digitalWrite(stepPin, HIGH);
            delayMicroseconds(stepDuration);
            digitalWrite(stepPin, LOW);
            delayMicroseconds(stepDuration);
  }
  while(true){
            digitalWrite(stepPin, LOW);
            digitalWrite(dirPin, LOW);
            }
}
```